Structural Engineering and Mechanics, *Vol. 51, No. 6 (2014) 955-971*
DOI: http://dx.doi.org/10.12989/sem.2014.51.6.955

Large post-buckling behavior of Timoshenko beams under axial compression loads

Şeref D. Akbaş*

Department of Civil Engineering, Bursa Technical University, Yıldırım Campus, 152 Evler Mah., Eğitim Cad., 1. Damla Sok., No:2/10, 16330 Yıldırım, Bursa, Turkey

(Received January 9, 2014, Revised April 11, 2014, Accepted May 18, 2014)

Abstract. Large post-buckling behavior of Timoshenko beams subjected to non-follower axial compression loads are studied in this paper by using the total Lagrangian Timoshenko beam element approximation. Two types of support conditions for the beams are considered. In the case of beams subjected to compression loads, load rise causes compressible forces end therefore buckling and post-buckling phenomena occurs. It is known that post-buckling problems are geometrically nonlinear problems. The considered highly non-linear problem is solved considering full geometric non-linearity by using incremental displacement-based finite element method in conjunction with Newton-Raphson iteration method. There is no restriction on the magnitudes of deflections and rotations in contradistinction to von-Karman strain displacement relations of the beam. The beams considered in numerical examples are made of lower-Carbon Steel. In the study, the relationships between deflections, rotational angles, critical buckling loads, post-buckling configuration, Cauchy stress of the beams and load rising are illustrated in detail in post-buckling case.

Keywords: gometrical non-linearity; post-buckling analysis; total Lagrangian finite element model; timoshenko beam; large displacements; large rotations

1. Introduction

Buckling or post-buckling is occurred by a sudden failure of a structural member subjected to high compressive loads. Understanding the buckling and post-buckling mechanism of structural elements is very important. It is known that buckling and post-buckling problems are geometric nonlinear problems. In recent years, with the development of technology in aerospace engineering, structural engineering, robotics and manufacturing make it inevitable to excessively use non-linear models that must be solved numerically. Because, closed-form solutions of geometrically nonlinear problems of beams with general loading and boundary conditions using elliptic integrals are limited. In the literature, studies of the post-buckling of beams under axial compressive loads are as follows; Nakashima *et al*. (1983) studied buckling and post-buckling behavior of steel beam-columns. Wu (1995) investigated shear deformation on the buckling behavior of a beam supported laterally by a Winkler elastic foundation. Kounadis and Ioannidis (1994) examined

*Corresponding author, Assistant Professor, E-mail: serefda@yahoo.com, seref.akbas@btu.edu.tr

http://www.techno-press.org/?journal=sem&subpage=8 ISSN: 1225-4568 (Print), 1598-6217 (Online)

elastic lateral postbuckling response of geometrically perfect beams, under simultaneously uniform bending and axial compression. Moradi and Taheri (1999) present the postbuckling response of a one-dimensional delaminated composite beam under axial compression by using differential quadrature method. Post-buckling behavior of poroelastic columns subjected to axial compressive forces is investigated by Cederbaum (2000). Ji and Hansen (2000) examined the non-linear response of a clamped-sliding postbuckled beam subjected to a harmonic axial load. Dado *et al*. (2004) studied post-buckling problem of a fixed-free column composed of two segments connected by a linear rotational spring with different flexural stiffness and lengths. Zyczkowski (2004) analyzed the effects of behaviour of loading during the buckling process on the value of critical force and initial stability of post-buckling path for elastic, non-prismatic columns. Li and Zhou (2005) examined geometrically non-linear theory for extensible elastic beams, governing equations of statically post-buckling of a beam with one end hinged and the other fixed, subjected to a uniformly distributed. Kounadis (2006) investigated lateral postbuckling response of thin-walled structures such as bars and frames with members having steel rolled shapes as well as circular cylindrical shells under axial compression. Aristizabal-Ochoa (2007) studied nonlinear large deflection-small strain analysis and postbuckling behavior of Timoshenko beam-columns of symmetrical cross section with semi-rigid connections subjected to conservative and non-conservative end loads. Nayfeh and Emam (2008) investigated an exact solution for the postbuckling configurations of beams with fixed-fixed, fixed-hinged, and hinged-hinged boundary conditions taking into account the geometric nonlinearity arising from midplane stretching. Challamel (2011) investigated post-buckling of an axially loaded elastic beam resting on linearly elastic medium. Challmel (2012) studied geometrically exact elastic stability analysis of two interacting kinematically constrained, flexible columns. Dolecek *et al*. (2009) analyzed of beam elongation influence on the postbuckling displacements in case of axial compression by a force depending on axial deformation of the beam. Dourakopoulos and Sapountzakis (2010) present postbuckling analysis of beams of arbitrary cross section taking into account moderate large displacements, large angles of twist and adopting second order approximations for the deflection-curvature relations. Gupta *et al*. (2010) anlyzed simple, elegant, and accurate closed-form expressions for predicting the post-buckling behavior of composite beams with axially immovable ends using the Rayleigh-Ritz (R-R) method. Sepahi *et al*. (2010) investigated post-buckling analysis of variable cross-section cantilever beams under combined load by using differential quadrature method. Emam (2011) studied postbuckling response of composite beams modeled according to higher-order shear deformation theories. Kocatürk and Akbaş (2011) investigated post-buckling analysis of Timoshenko beams with various boundary conditions under non-uniform thermal loading by using total Lagrangian finite element approximation. Fallah and Aghdam (2011) studied and presented simple analytical expressions for large amplitude free vibration and post-buckling analysis of functionally graded beams rest on nonlinear elastic foundation subjected to axial force with using Von Karman's strain-displacement relation. Kocatürk and Akbaş (2012) present thermal post-buckling behavior of functionally graded Timoshenko beams by using the total Lagrangian Timoshenko beam element approximation. Saetiew and Chucheepsakul (2012a) studied post-buckling behavior of a linearly tapered column with pinned ends made of nonlinear elastic materials and subjected to an axial compressive force by using Ludwick constitutive law. Saetiew and Chucheepsakul (2012b) analyzed post-buckling behavior of a simply supported column made of nonlinear elastic materials subjected to an end axial force by using the shooting method. Large amplitude free vibration and thermal post-buckling of shear flexible Functionally Graded Material (FGM) beams is studied using finite element formulation based on first order

Timoshenko beam theory by Anandrao *et al*. (2012). Akbaş and Kocatürk (2012) analyzed post-Buckling behaviour of Timoshenko Beams with Temperature-Dependent Physical Properties under Uniform Thermal Loading. Yuan and Wang (2011) investigated buckling and post-buckling analysis of extensible beam-columns by using a new differential quadrature based iterative numerical integration method. is proposed to solve post-buckling differential equations of extensible beam-columns. Brojan and Kosel (2011) investigated post-buckling analysis of non-linearly elastic columns made of Ludwick material for free-clamped, hinged-hinged and clamped-clamped supports. Le Grognec and Le van (2011) examined elastoplastic buckling and post-buckling of Timoshenko beams under axial compression. Zhang and Murphy (2013) analyzed instability phenomenon in the post-buckling region. Zhu *et al*. (2011) presented nonlinear stability and post-buckling for Euler-type beam-column structures. Gundaand Rao (2013) investigated post-buckling analysis of composite beams with axially immovable ends using geometric nonlinearity of von-Karman type. Humer (2013) investigated buckling and postbuckling of beams taking into account both the influence of axial compressibility and shear deformation. Rahimi *et al*. (2013) investigated postbuckling behavior of functionally graded beams by using Von-Karman type nonlinear strain-displacement relationships.

It is seen from literature that that investigations of post-buckling of beams are limited within the full geometrically nonlinear analysis. It is seen from literature that the post-buckling studies of beams are investigated within von Karman nonlinear strain approximation in which full geometric non-linearity cannot be considered. In von Karman nonlinear strain approximation, because of neglect of some components of strain, satisfactory results can be obtained only for large displacements but moderate rotations. It is known that post-buckling problems are geometrically nonlinear problems. In the present study, the large post-buckling analysis of Timoshenko beams with various boundary conditions under non-follower axial compression loads is considered by using the total Lagrangian finite element method by taking into account full geometric nonlinearity. There is no restriction on the magnitudes of deflections and rotations in contradistinction to von-Karman strain displacement relations of the beam.

The considered highly non-linear problem is solved considering full geometric non-linearity by using incremental displacement-based finite element method in conjunction with Newton-Raphson iteration method. The distinctive feature of this study is large deflection static analysis Timoshenko beams considering full geometric non-linearity according to other studies which are investigated by using von-Karman strain displacement relations of the beam.

The development of the formulations of general solution procedure of nonlinear problems follows the general outline of the derivation given by Zienkiewicz and Taylor (2000). In deriving the formulations for geometrically nonlinear analysis of Timoshenko beams, the total Lagrangian Timoshenko beam element formulations for given by Felippa (2014) are used. The relationships between deflections, rotational angles, thermal post-buckling configuration, Cauchy stresses of the beams and temperature rising are illustrated in detail in post-buckling case.

2. Theory and formulations

The various beam configurations, made of isotropic, elastic material, with co-ordinate system O(X,Y,Z), considered in the present study are shown in Fig. 1. The beam is subjected to a non-follower compressive point load (P) at the end of the beam as seen from Fig. 1.

In this study, the Total Langragian Timoshenko beam element is used and the related

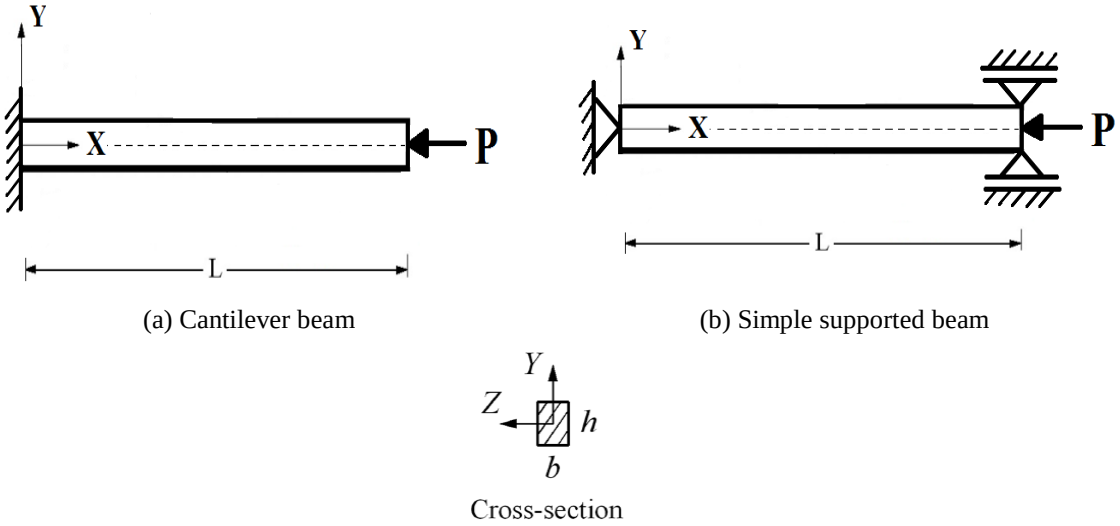

(a) Cantilever beam (b) Simple supported beam

Fig. 1 Beams with various boundary conditions subjected to a non-follower compressive point load (P) at the end of the beam and cross-section

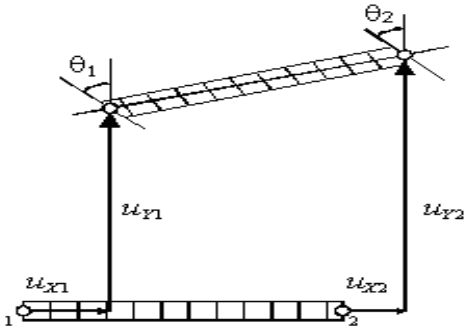

Fig. 2 A two-node C^0 beam element

formulations are developed by using the formulations given by Felippa (2014). In the present study, finite element model of Timoshenko beam element is developed by using a two-node beam element shown in Fig. 2. Each node has three degrees of freedom: Two node displacements u_{xi} and u_{yi}, and one rotation θ_i about Z axis.

A particle originally located at $P_0(X,Y)$ moves to $P(x,y)$ in the current configuration, as shown in Fig. 3. The projections of P_0 and P along the cross sections at C_0 and C upon the neutral axis are called $C_0(X,0)$ and $C(x_c,y_c)$, respectively. It will be assumed that dimensions of the beam cross section do not change, and that the shear distortion γ<<1 so that cosγ can be replaced by 1 (Felippa 2014).

$$x = x_c - Y(\sin\psi + \sin\gamma\cos\psi) = x_c - Y[\sin(\psi+\gamma) + (1-\cos\gamma)\sin\psi] = x_c - Y\sin\theta \quad (1)$$

$$y = y_c + Y(\cos\psi - \sin\gamma\sin\psi) = y_c + Y[\cos(\psi+\gamma) + (1-\cos\gamma)\cos\psi] = y_c + Y\cos\theta \quad (2)$$

where x_c=X+u_{XC} and y_c=u_{XC}. Consequently, x=X+u_{XC}−Ysinθ and y=u_{YC}+Ycosθ. From now on we

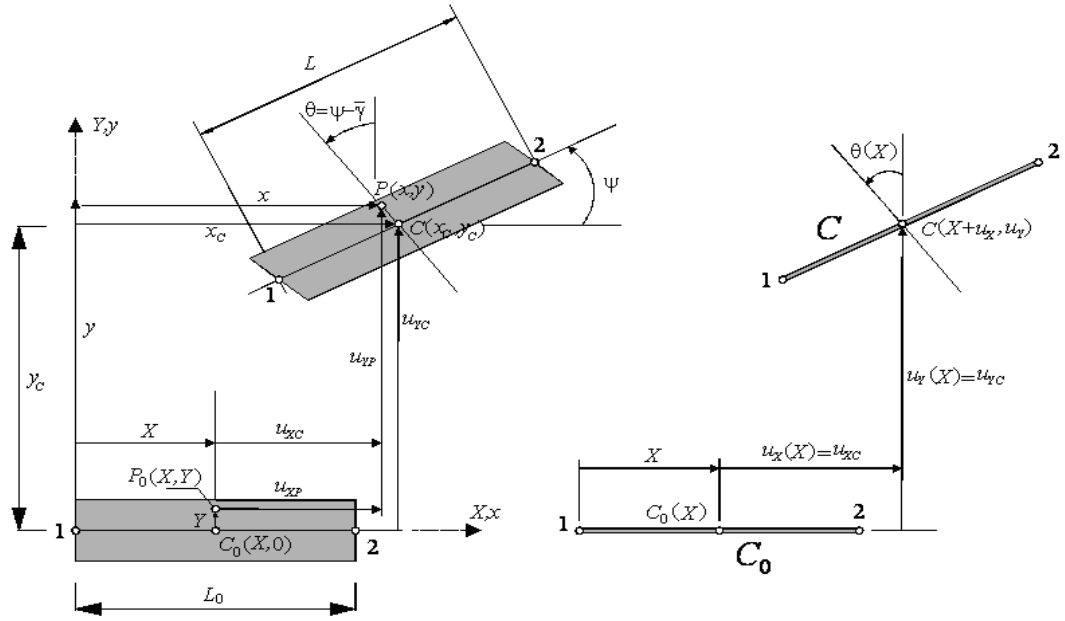

Fig. 3 Lagrangian kinematics of the C_0 beam element with X-aligned reference configuration (a) plane beam moving as a two-dimensional body (b) reduction of motion description to one dimension measured by coordinate X. This figure is given by Felippa (2014)

shall call u_{XC} and u_{YC} simply u_X and u_Y, respectively, so that the Lagrangian representation of the motion is

$$\begin{bmatrix} x \\ y \end{bmatrix} = \begin{bmatrix} X + u_X - Y\sin\theta \\ u_Y + Y\cos\theta \end{bmatrix} \tag{3}$$

in which u_X, u_Y and θ are functions of X only. This concludes the reduction to a one-dimensional model, as sketched in Fig. 3(b). For a two-node C_0 element, it is natural to express the displacements and rotation functions as linear in between the node displacements

$$\mathbf{w} = \begin{bmatrix} u_X(X) \\ u_Y(X) \\ \theta(X) \end{bmatrix} = \frac{1}{2}\begin{bmatrix} 1-\xi & 0 & 0 & 1+\xi & 0 & 0 \\ 0 & 1-\xi & 0 & 0 & 1+\xi & 0 \\ 0 & 0 & 1-\xi & 0 & 0 & 1+\xi \end{bmatrix} \begin{bmatrix} u_{X1} \\ u_{Y1} \\ \theta_1 \\ u_{X2} \\ u_{Y2} \\ \theta_2 \end{bmatrix} = \mathbf{N}\mathbf{u} \tag{4}$$

in which $\xi=(2X/L_0)-1$ is the isoparametric coordinate that varies from $\xi=-1$ at node 1 to $\xi=1$ at node 2.

The Green-Lagrange strains are given as follows Felippa (2014)

$$[\mathbf{e}]=\begin{bmatrix} e_1 \\ e_2 \end{bmatrix}=\begin{bmatrix} e_{XX} \\ 2e_{XY} \end{bmatrix}=\begin{bmatrix} (1+u_X^{'})\cos\theta+u_Y^{'}\sin\theta-Y\theta^{'}-1 \\ -(1+u_X^{'})\sin\theta+u_Y^{'}\sin\theta \end{bmatrix}+=\begin{bmatrix} e-Y\kappa \\ \gamma \end{bmatrix} \tag{5}$$

$$e=(1+u_X^{'})\cos\theta+u_Y^{'}\sin\theta-1;\ \gamma=-(1+u_X^{'})\sin\theta+u_Y^{'}\sin\theta;\ \kappa=\theta^{'} \tag{6}$$

where e is the axial strain, γ is the shear strain and κ is curvature of the beam, $u'_X=du_X/dX$, $u'_Y=du_Y/dX$, $\theta'=d\theta/dX$.

According to Hooke's law, constitutive equations of the beam with the second Piola-Kirchhoff stresses are as follows

$$s=\begin{bmatrix} S_{XX} \\ S_{XY} \end{bmatrix}=\begin{bmatrix} s_1 \\ s_2 \end{bmatrix}=\begin{bmatrix} s_1^0+Ee_1 \\ s_2^0+Ge_2 \end{bmatrix} \tag{7}$$

where s^0_1, s^0_2 are initial stresses, E is the modulus of elasticity, G is the shear modulus. Using constitutive equations, axial force N, shear force V and bending moment M can be obtained as

$$N=\int_A s_1 dA=\int_A [s_1^0+Ee_1]dA=N^0+Ee_1A \tag{8}$$

$$V=\int_A s_2 dA=\int_A [s_2^0+Ge_2]dA=V^0+GA\gamma \tag{9}$$

$$M=\int_A -Ys_1 dA=\int_A -Y[s_1^0+Ee_1]dA=M^0+EI_0\kappa \tag{10}$$

where

$$N^0=\int_{A_0} s_1^0 dA,\ \ V^0=\int_{A_0} s_2^0 dA,\ \ M^0=\int_{A_0} -Ys_1^0 dA \tag{11}$$

For the solution of the total Lagrangian formulations of Timoshenko beam problem, small-step incremental approaches from known solutions are used. As it is known, it is possible to obtain solutions in a single increment of the external force only in the case of mild nonlinearity (and no path dependence). To obtain realistic answers, physical insight into the nature of the problem and, usually, small-step incremental approaches from known solutions are essential. Such incremental procedures are useful to reduce excessive numbers of iterations and in following the physically correct path. In the iterations, the load is divided by a suitable number according to the value of load. The loading is divided by large numbers. After completing an iteration process, the load is increased by adding load increment to the accumulated load.

In this study, small-step incremental approaches from known solutions with Newton-Raphson iteration method are used in which the solution for n+1 th load increment and i th iteration is obtained in the following form

$$d\,\mathbf{u}_n^i = (\mathbf{K}_T^i)^{-1}\mathbf{R}_{n+1}^i \tag{12}$$

where (K_T^i) is the system stiffness matrix corresponding to a tangent direction at the i th iteration, $d\,\mathbf{u}_n^i$ is the solution increment vector at the i th iteration and n+1 th load increment, $(R_{n+1}^i)_S$ is the system residual vector at the i th iteration and $n+1$ th load increment. This iteration

procedure is continued until the difference between two successive solution vectors is less than a selected tolerance criterion in Euclidean norm given by

$$\sqrt{\frac{[(d\mathbf{u}_n^{i+1}-d\mathbf{u}_n^{i})^T(d\mathbf{u}_n^{i+1}-d\mathbf{u}_n^{i})]^2}{[(d\mathbf{u}_n^{i+1})^T(d\mathbf{u}_n^{i+1})]^2}} \le \varsigma_{tol} \tag{13}$$

A series of successive approximations gives

$$\mathbf{u}_{n+1}^{i+1} = \mathbf{u}_{n+1}^{i} + d\mathbf{u}_{n+1}^{i} = \mathbf{u}_n + \Delta\mathbf{u}_n^{i} \tag{14}$$

where

$$\Delta\mathbf{u}_n^{i} = \sum_{k=1}^{i} d\mathbf{u}_n^{k} \tag{15}$$

The residual vector R_{n+1}^{i} for a finite element is as follows

$$\mathbf{R}_{n+1}^{i} = \mathbf{f} - \mathbf{p} \tag{16}$$

where **f** is the vector of external forces and **p** is the vector of internal forces given in Appendix.

The element tangent stiffness matrix for the total Lagrangian Timoshenko plane beam element is as follows which is given by Felippa (2014)

$$\mathbf{K}_T = \mathbf{K}_M + \mathbf{K}_G \tag{17}$$

where $\mathbf{K}_G$ is the geometric stiffness matrix, and $\mathbf{K}_M$ is the material stiffness matrix given as follows by Felippa (2014)

$$\mathbf{K}_M = \int_{L_0} \mathbf{B}_m^T \mathbf{S} \mathbf{B}_m dX \tag{18}$$

The explicit forms of the expressions in Eq. (17) is given in Appendix. After integration of Eq. (18), K_M can be expressed as follows

$$\mathbf{K}_M = \mathbf{K}_M^a + \mathbf{K}_M^b + \mathbf{K}_M^s \tag{19}$$

where $\mathbf{K}_M^a$ is the axial stiffness matrix, $\mathbf{K}_M^b$ is the bending stiffness matrix, $\mathbf{K}_M^s$ is the shearing stiffness matrix and explicit forms of these expressions are given in Appendix. The geometric stiffness matrix K_G, $\mathbf{B}_m$ and the internal nodal force vector **p** remain given in Appendix.

After obtaining the displacements of nodes, the second Piola-Kirchhoff stress tensor components S_{xx}, S_{xy}, S_{yy} can be obtained by using Eq. (7). It is known that the relation between the Cauchy stress tensor components σ_{xx}, σ_{yy}, σ_{xy} and the second Piola-Kirchhoff stress tensor components S_{xx}, S_{xy}, S_{yy} can be written as follows

$$\sigma_{xx} = \frac{^2\rho}{_0\rho}\left(\frac{\partial x}{\partial X}\frac{\partial x}{\partial X}S_{xx} + 2\frac{\partial x}{\partial X}\frac{\partial x}{\partial Y}S_{xy} + \frac{\partial x}{\partial Y}\frac{\partial x}{\partial Y}S_{yy}\right) \tag{20a}$$

$$\sigma_{yy}=\frac{{}^{2}\rho}{{}^{0}\rho}\left(\frac{\partial y}{\partial X}\frac{\partial y}{\partial X}S_{xx}+2\frac{\partial y}{\partial X}\frac{\partial y}{\partial Y}S_{xy}+\frac{\partial y}{\partial Y}\frac{\partial y}{\partial Y}S_{yy}\right) \tag{20b}$$

$$\sigma_{xy}=\frac{{}^{2}\rho}{{}^{0}\rho}\left(\frac{\partial x}{\partial X}\frac{\partial x}{\partial X}S_{xx}+2\frac{\partial x}{\partial X}\frac{\partial y}{\partial Y}S_{xy}+\frac{\partial x}{\partial Y}\frac{\partial x}{\partial Y}S_{yy}\right) \tag{20c}$$

where ${}^{0}\rho$ and ρ represent the mass densities of the material in configurations C_0 and C, respectively. The relations between the Lagrange coordinates X,Y and Euler coordinates x,y are given by Eqs. (1), (2). The relation between ${}^{0}\rho$ and ρ is as follows;

The relation between ${}^{0}\rho$ and ρ is as follows

$${}^{0}\rho=\rho J \tag{21}$$

where J is the determinant of the deformation gradient tensor **F** (or the Jacobian of the transformation) and defined as follows

$$J=\det(\mathbf{F})=\begin{vmatrix}\frac{\partial x}{\partial X} & \frac{\partial x}{\partial Y} & \frac{\partial x}{\partial Z}\\ \frac{\partial y}{\partial X} & \frac{\partial y}{\partial Y} & \frac{\partial y}{\partial Z}\\ \frac{\partial z}{\partial X} & \frac{\partial z}{\partial Y} & \frac{\partial z}{\partial Z}\end{vmatrix} \tag{22}$$

In this study, it is assumed that ${}^{0}\rho=\rho$.

3. Numerical results

In the numerical examples, the post-buckling deflections as well as the max. Cauchy normal stresses, thermal post-buckling configuration, critical buckling temperatures, end rotational angles are calculated and presented in figures for different compressive loads. To this end, by use of usual assembly process, the system tangent stiffness matrix and the system residual vector are obtained by using the element stiffness matrixes and element residual vectors for the total Lagrangian Timoshenko plane beam element. After that, the solution process outlined in the previous section is used for obtaining the related solutions for the total Lagrangian finite element model of Timoshenko plane beam element. The beams considered in numerical examples are made of lower-carbon Steel: E=70 GPa, ν=0.2875. In the numerical integrations, five-point Gauss integration rule is used. In the numerical calculations, the number of finite elements is taken as n=100. Unless otherwise stated, it is assumed that the the height of the beam is h=1 m, the width of the beam is b=1 m and length of the beam is L=3 m in the numerical results. In the post-buckling case, the Cauchy stresses can be obtained by using Eqs. (20a-c) after obtaining the second Piola-Kirchhoff stresses by using Eq. (7).

In Fig. 4 critical buckling compressive loads (P_{CR}) versus the ratio L/h (Length/height) of the beam is compared with Euler Bernoulli beam theory and Timoshenko beam theory. For calculating of Euler Bernoulli beam theory, the Euler formula is used ($P_{cr}=\pi^2 EI/L^2{}_b$).

It is clearly seen from Fig. 4 that, with decrease in the ratio L/h, the difference between the results of Euler Bernoulli beam theory and Timoshenko beam theory differs considerably. This

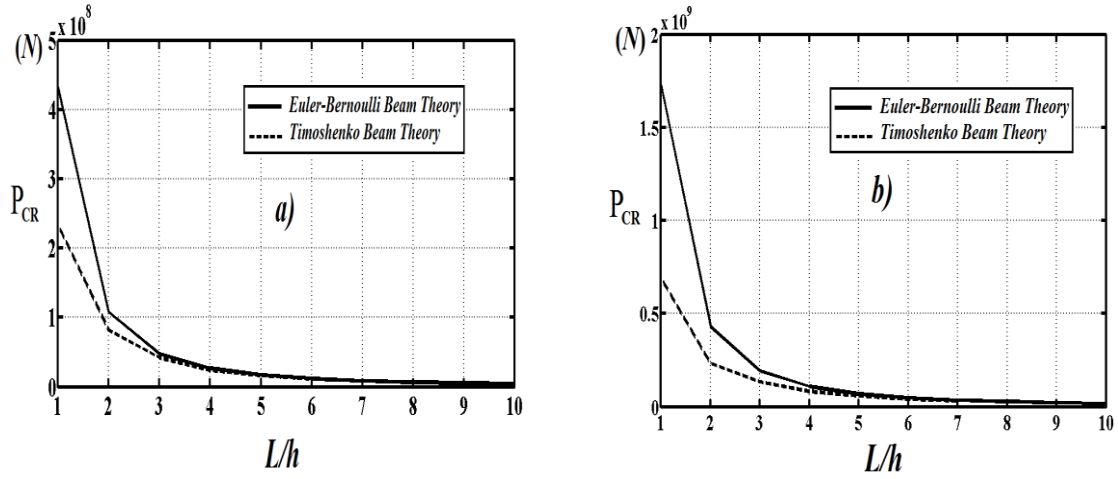

Fig. 4 Critical buckling compressive loads (P_{CR}) the ratio *L/h* (Length/height) of the beam for Euler Bernoulli beam theory and Timoshenko beam theory (a) Cantilever beam (b) Simple supported beam

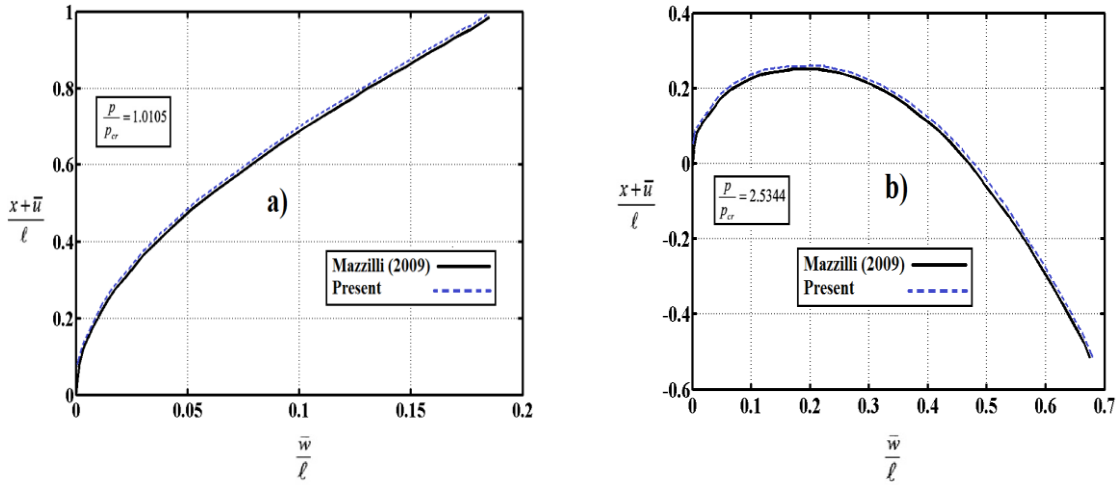

Fig. 5 Post-buckled configurations for (a) p/p_{cr}=1.0105 and (b) p/p_{cr}=2.5344

difference based on that the effect of the shear stresses on the deformation in the Timoshenko beam theory. This is because, with decrease in the ratio *L/h*, the shear stresses increases in the beam. Therefore, for the ratio *L/h*, Timoshenko beam theory must be used instead of Euler Bernoulli beam theory.

In order to establish the accuracy of the present formulation and the computer program developed by the author, the results obtained from the present study are compared with the available results in the literature. For this purpose, the post-buckling configurations of a cantilever beam with different loads (normalized loads and displacements) are plotted and compared with data presented in Fig. 4(a) and Fig. 4(d) of Mazzilli (2009).

It is clearly seen that Fig. 5 that the curves of the present study are very close to those of Mazzilli (2009).

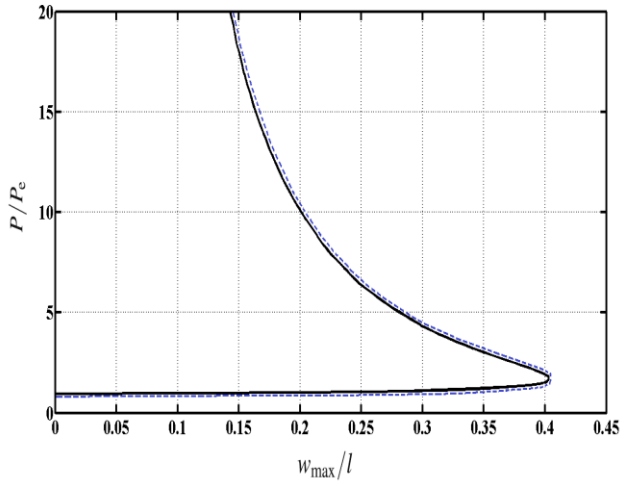

Fig. 6 Load-deflection curves of a simply supported beam

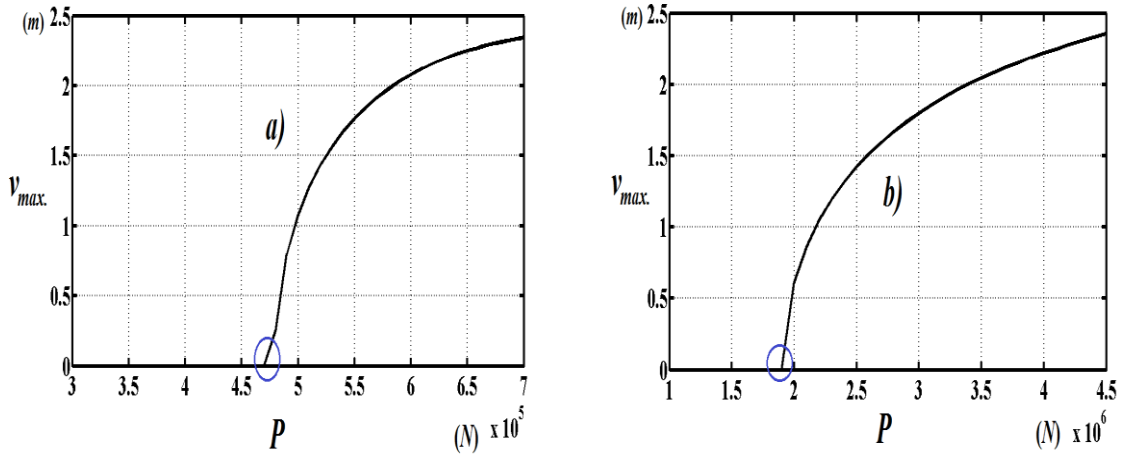

Fig. 7 Load-the maximum vertical displacements curves rising compressive loads (a) Cantilever beam (b) Simple supported beam

To further verify the present results, for a simple supported beam, the maximum deflection versus compressive forces are plotted and compared with those of Fig. 8(a) of Humer (2013).

Comparisons of Fig. 6 with Fig. 8(a) of Humer (2013) show that there is a perfect harmony between the present results and those of Humer (2013).

In Figs. 7, 8 and 9, the maximum vertical displacements, maximum rotational angles θ (rad.) and maximum Cauchy normal stresses versus load rising are presented. For locations of maximum vertical displacement; the free end of the beam is taken in the cantilever beam and the midpoint of the beam is taken simple supported beam. For locations of maximum rotational angles θ (rad.); the free end of the beam is taken in the cantilever beam and the left end of the beam is taken in the simple supported beam. For locations of maximum Cauchy normal stresses; the left end of the beam is taken in the cantilever beam and the midpoint of the beam is taken simple supported beam.

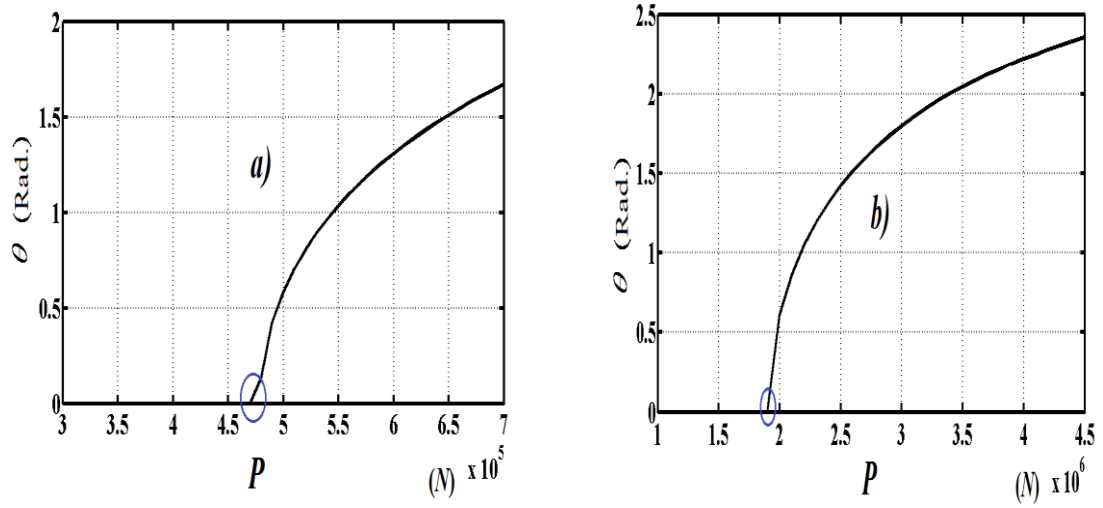

Fig. 8 Load-the maximum rotational angles curves rising compressive loads (a) Cantilever beam (b) Simple supported beam

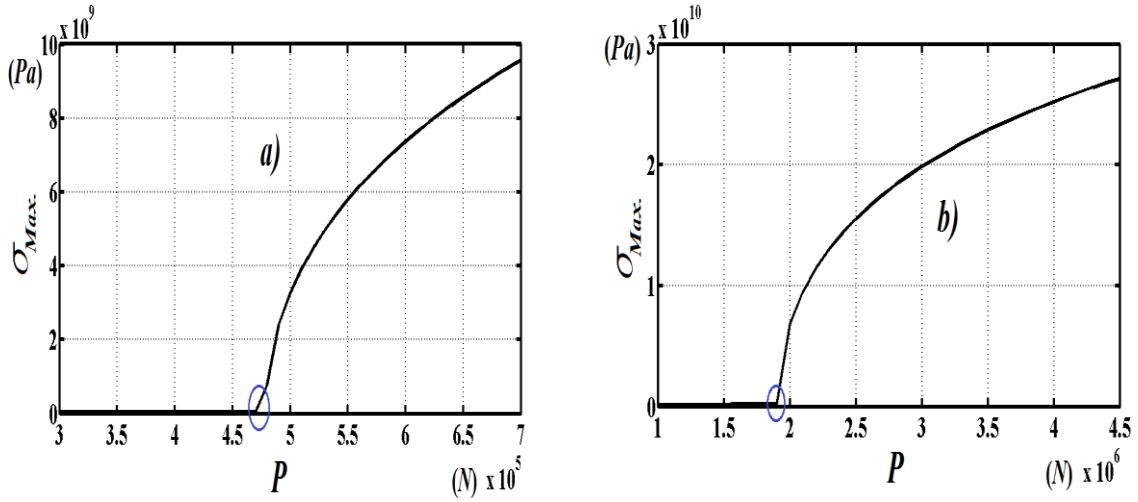

Fig. 9 Load-the maximum Cauchy normal stresses curves rising compressive loads (a) Cantilever beam (b) Simple supported beam

In Figs. 7, 8 and 9, furcation points can be seen (see circle). As it is known, buckling occurs at the furcation points: Actually these points are bifurcation points. As it is known, according to the initial arbitrary deviation from the straight position of the beam, buckling can occur in either positive or negative directions. In this study, deviation from the straight position is always taken as positive for buckling analysis. The symmetrical branches according to load axis would be obtained if the deviations from the straight positions were taken as negative values. It is seen Figs. 7, 8 and 9 that with increase in load, the responses of the beams converge. This situation may be explained as follows: the arm of the external forces change with the magnitude of the external force and, as the magnitude of the force increases the arm of these external forces decrease. However, as the

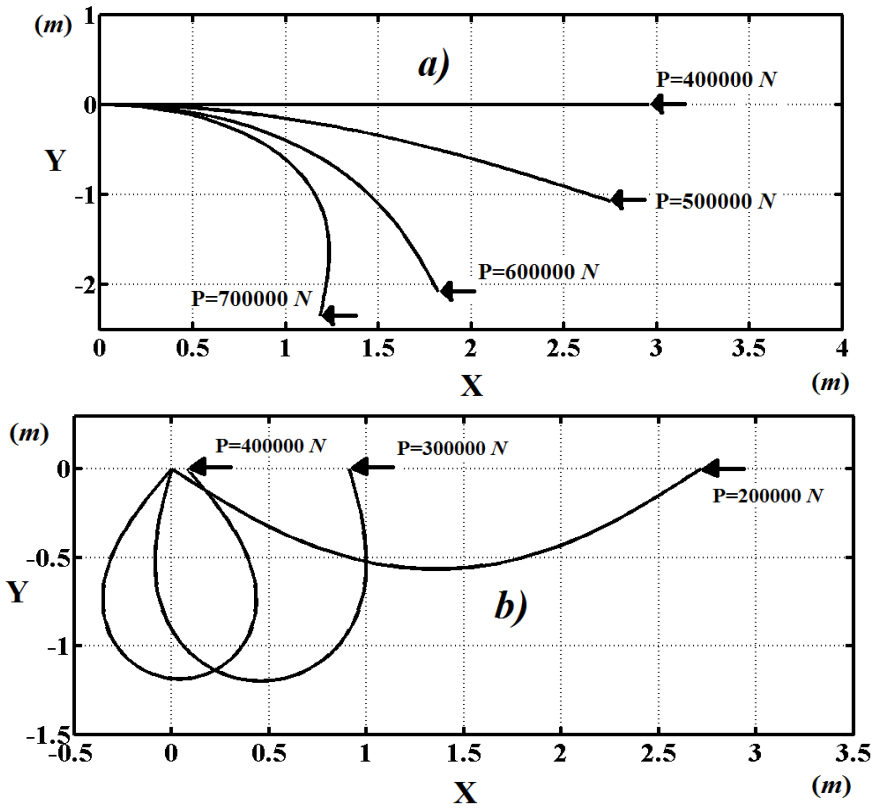

Fig. 10 Post-buckling configuration of the beams for different compressive loads (a) Cantilever beam (b) Simple supported beam

forces increase the configuration of the beam become close to vertical direction and therefore increase in the load does not cause a significant increase in displacements after certain load level in which the configuration of the beam is close to the vertical direction. This situation is seen in Fig. 10 which shows the displaced configuration of the beam. After this load, it is expected that axial rigidity of the beam gains more importance than its flexural rigidity.

Fig. 10 displays the post-buckling configuration of the beam for different compressive loads.

It is seen from figure 10 that after buckling loads, the configuration of the beams change considerably. By using full geometrically nonlinear model, it is calculated and presented more realistic mechanical behaviors of structures.

4. Conclusions

This paper focuses on post-buckling analysis of Timoshenko beams with various boundary conditions subjected to a compressive loading by using the total Lagrangian Timoshenko beam element approximation. Two type of support conditions for the beams are considered. The considered highly non-linear problem is solved by using incremental displacement-based finite element method in conjunction with Newton-Raphson iteration method. The relationships between

deflections, end rotational angles, critical buckling loads, post-buckling configuration, Cauchy stress of the beams and load rising are illustrated in detail in post-buckling case. In this study, the post buckling analysis of Timoshenko beams under compressive loading with various boundary conditions is considered by using total Lagrangian finite element method in which full geometric nonlinearity can be considered as distinct from the literature studies. Future work should be devoted to the interpretation of the results in order to develop post-buckling behavior of beams. The superiority or advantage of the finite element method to the other methods is that in the finite element method, all the boundary conditions can be taken into consideration without any difficulty. It is seen from results that learn about more realistic post-buckling behaviour of the beams, full the geometrically non-linear model must be considered.

References

Akbaş, Ş.D. and Kocatürk, T. (2012), "Post-buckling analysis of Timoshenko beams with temperature-dependent physical properties under uniform thermal loading", *Struct. Eng. Mech.*, **44**(1), 109-125.

Anandrao, K.S., Gupta, R.K., Ramchandran, P. and Rao, G.V. (2012), "Non-linear free vibrations and post-buckling analysis of shear flexible functionally graded beams", *Struct. Eng. Mech.*, **44**(3), 339-361.

Aristizabal-Ochoa, J.D. (2007), "Large deflection and postbuckling behavior of Timoshenko beam-columns with semi-rigid connections including shear and axial effects", *Eng. Struct.*, **29**(6), 991-1003

Brojan, M. and Kosel, F. (2011), "Approximative formula for post-buckling analysis of non-linearly elastic columns with superellipsoidal cross-sections", *J. Reinf. Plast. Compos.*, **30**(5), 409-415.

Cederbaum, G. (2000), "Post-buckling behavior of poroelastic columns", *Int. J. Mech. Sci.*, **42**(4), 771-783.

Challamel, N. (2011), "On the post-buckling of elastic beams on gradient foundation", *Compt. Rend. Mecanique*, **339**(6), 396-405.

Challamel, N. (2012), "On geometrically exact post-buckling of composite columns with interlayer slip-The partially composite elastica", *Int. J. Nonlin. Mech.*, **47**(3), 7-17.

Dado, M., Al-Sadder, S. and Abuzeid, O. (2004), "Post-buckling behavior of two elastica columns linked with a rotational spring", *Int. J. Nonlin. Mech.*, **39**(10), 1579-1587.

Dolecek, V., Isic, S. and Voloder, A. (2009), "An analysis of beam elongation influence to postbuckling displacements under displacement dependent axial force", *Mechanika*, **4**, 25-30.

Dourakopoulos, J.A. and Sapountzakis, E.J. (2010), "Postbuckling analysis of beams of arbitrary cross section using BEM", *Eng. Struct.*, **32**(11), 3713-3724.

Emam, S.A. (2011), "Analysis of shear-deformable composite beams in postbuckling", *Compos. Struct.*, **94**(1), 24-30.

Fallah, A. and Aghdam, M.M. (2011), "Nonlinear free vibration and post-buckling analysis of functionally graded beams on nonlinear elastic foundation", *Eur. J. Mech. A-Solid.*, **30**(4), 571-583.

Felippa, C.A. (2014), Notes on Nonlinear Finite Element Methods, http://www.colorado.edu/engineering/cas/courses.d/NFEM.d/NFEM.Ch10.d/NFEM.Ch10.pdf, Retrieved January.

Gunda, J.B. and Rao, G.V. (2013), "Post-buckling analysis of composite beams: a simple intuitive formulation", *Sadhana-Academy Proceedings In Engineering*, **38**(3), 447-459.

Gupta, R.K., Gunda, J.B., Janardhan, G.R. and Rao, G.V. (2010), "Post-buckling analysis of composite beams: Simple and accurate closed-form expressions", *Compos. Struct.*, **92**(8), 1947-1956.

Humer, A. (2013), "Exact solutions for the buckling and postbuckling of shear-deformable beams", *ACTA Mechanika*, **224**(7), 1493-1525.

Ji, J.C. and Hansen, C.H. (2000), "Non-linear response of a post-buckled beam subjected to a harmonic axial excitation", *J. Sound Vib.*, **237**(2), 303-318.

Kocatürk, T. and Akbaş, Ş.D. (2011), "Post-buckling analysis of Timoshenko beams with various boundary

conditions under non-uniform thermal loading", *Struct. Eng. Mech.*, **40**(3), 347-371.
Kocatürk, T. and Akbaş, Ş.D. (2012), "Post-buckling analysis of Timoshenko beams made of functionally graded material under thermal loading", *Struct. Eng. Mech.*, **41**(6), 775-789.
Kounadis, A.N. and Ioannidis, G.I. (1994), "Lateral postbuckling analysis of beam-columns", *J. Eng. Mech.*, ASCE, **120**(4), 695-706.
Kounadis, A.N. (2006), "Recent advances on postbuckling analyses of thin-walled structures: Beams, frames and cylindrical shells", *J. Construct. Steel Res.*, **62**(11), 1101-1115.
Le Grognec, P. and Le van, A. (2011), "On the plastic bifurcation and post-bifurcation of axially compressed beams", *Int. J. Nonlin. Mech.*, **46**(5), 693-702.
Li, S.R. and Zhou, Y. (2005), "Post-buckling of a hinged-fixed beam under uniformly distributed follower forces", *Mech. Res. Commun.*, **32**(4), 359-367.
Mazzilli, C.E.N. (2009), "Buckling and post-buckling of extensible rods revisited: A multiple-scale solution", *Int. J. Nonlin. Mech.*, **44**, 200-208.
Moradi, S. and Taheri, F. (1999), "Postbuckling analysis of delaminated composite beams by differential quadrature method", *Compos. Struct*., **46**(1), 33-39.
Nakashima, M., Nakamura, T. And Wakabayashi, M. (1983), "Post-Buckling Instability of Steel Beam-Columns", *J. Struct. Eng.*, ASCE, **109**(6), 1414-1430.
Nayfeh, A.H. and Emam, S.A. (2008), "Exact solution and stability of postbuckling configurations of beams", *Nonlin. Dyn.*, **54**(4), 395-408.
Rahimi, G.H., Gazor, M.S., Hemmatnezhad, M. and Toorani, H. (2013), "On the postbuckling and free vibrations of FG Timoshenko beams", *Compos. Struct.*, **95**, 247-253.
Saetiew, W. and Chucheepsakul, S. (2012a), "Post-buckling of linearly tapered column made of nonlinear elastic materials obeying the generalized Ludwick constitutive law", *Int. J. Mech. Sci.*, **65**(1), 83-96.
Saetiew, W. and Chucheepsakul, S. (2012b), "Post-buckling of simply supported column made of nonlinear elastic materials obeying the generalized Ludwick constitutive law", *Zamm-Zeitschrift Fur Angewandte Mathematik Und Mechanik*, **92**(6), 479-489.
Sepahi, O., Forouzan, M.R. and Malekzadeh, P. (2010), "Post-buckling analysis of variable cross-section cantilever beams under combined load via differential quadrature method", *Ksce J. Civil Eng.*, **14**(2), 207-214.
Wu, B. (1995), "Influence of shear deformation on the buckling of elastically supported beams", *Arch. Appl. Mech.*, **65**(3), 133-141.
Yuan, Z. and Wang, X. (2011), "Buckling and post-buckling analysis of extensible beam-columns by using the differential quadrature method", *Comput. Math. Appl.*, **62**(12), 4499-4513.
Zhang, Y. and Murphy, K.D. (2013), "Jumping instabilities in the post-buckling Of a beam on a partial nonlinear foundation", *Acta Mechanica Solida Sinica*, **26**(5), 500-513.
Zhu, Y.Y., Hu, Y.J. and Cheng, C.J. (2011), "Analysis of nonlinear stability and post-buckling for Euler-type beam-column structure", *Appl. Math. Mech.-English Edition*, **32**(6), 719-728.
Zyczkowski, M. (2004), "Post-buckling analysis of non-prismatic columns under general behaviour of loading", *Int. J. Nonlin. Mech.*, **40**(4), 445-463.
Zienkiewichz, O.C. and Taylor, R.L. (2000), *The Finite Element Method*, Fifth Edition, Volume 2: Solid, Mechanics, Butterworth-Heinemann, Oxford.

Appendix

The components of the material stiffness matrix: the axial stiffness matrix $\mathbf{K}_M^a$, the bending stiffness matrix $\mathbf{K}_M^b$ and the shearing stiffness matrix $\mathbf{K}_M^s$ are as follows

$$K_M^a=\frac{EA}{L_0}\begin{bmatrix} c_m^2 & c_m s_m & -c_m\gamma_m L_0/2 & -c_m^2 & -c_m s_m & -c_m\gamma_m L_0/2 \\ c_m s_m & s_m^2 & \gamma_m L_0 s_m/2 & -c_m s_m & -s_m^2 & -\gamma_m L_0 s_m/2 \\ -c_m\gamma_m L_0/2 & -\gamma_m L_0 s_m/2 & \gamma_m^2 L_0^2/4 & c_m\gamma_m L_0/2 & \gamma_m L_0 s_m/2 & \gamma_m^2 L_0^2/4 \\ -c_m^2 & -c_m s_m & c_m\gamma_m L_0/2 & c_m^2 & c_m s_m & c_m\gamma_m L_0/2 \\ -c_m s_m & -s_m^2 & \gamma_m L_0 s_m/2 & c_m s_m & s_m^2 & \gamma_m L_0 s_m/2 \\ -c_m\gamma_m L_0/2 & -\gamma_m L_0 s_m/2 & \gamma_m^2 L_0^2/4 & c_m\gamma_m L_0/2 & \gamma_m L_0 s_m/2 & \gamma_m^2 L_0^2/4 \end{bmatrix} \tag{A1}$$

$$K_M^b=\frac{EI_0}{L_0}\begin{bmatrix} 0 & 0 & 0 & 0 & 0 & 0 \\ 0 & 0 & 0 & 0 & 0 & 0 \\ 0 & 0 & 1 & 0 & 0 & -1 \\ 0 & 0 & 0 & 0 & 0 & 0 \\ 0 & 0 & 0 & 0 & 0 & 0 \\ 0 & 0 & -1 & 0 & 0 & 1 \end{bmatrix} \tag{A2}$$

$$K_M^s=\frac{GA}{L_0}\begin{bmatrix} s_m^2 & -c_m s_m & -\alpha_1 L_0 s_m/2 & -s_m^2 & c_m s_m & -\alpha_1 L_0 s_m/2 \\ -c_m s_m & c_m^2 & c_m\alpha_1 L_0/2 & c_m s_m & -c_m^2 & c_m\alpha_1 L_0/2 \\ -\alpha_1 L_0 s_m/2 & c_m\alpha_1 L_0/2 & \alpha_1^2 L_0^2/4 & \alpha_1 L_0 s_m/2 & -c_m\alpha_1 L_0/2 & \alpha_1^2 L_0^2/4 \\ -s_m^2 & c_m s_m & \alpha_1 L_0 s_m/2 & s_m^2 & -c_m s_m & \alpha_1 L_0 s_m/2 \\ c_m s_m & -c_m^2 & -c_m\alpha_1 L_0/2 & -c_m s_m & c_m^2 & -c_m\alpha_1 L_0/2 \\ -\alpha_1 L_0 s_m/2 & c_m\alpha_1 L_0/2 & \alpha_1^2 L_0^2/4 & \alpha_1 L_0 s_m/2 & -c_m\alpha_1 L_0/2 & \alpha_1^2 L_0^2/4 \end{bmatrix} \tag{A3}$$

where m stands for beam midpoint, $\xi=0$, and $\theta_m=(\theta_1+\theta_2)/2$, $\omega_m=\theta_m+\varphi$, $c_m=\cos\omega_m$, $s_m=\sin\omega_m$, $e_m=L\cos(\theta_m-\psi)/L=-1$, $\alpha_1=1+e_m$ and $\gamma_m=L\sin(\psi-\theta_m)/L_0$ (See Fig. A1 for symbols). The axis of the considered beam initially is taken as horizontal, therefore $\varphi=0$. The matrix **S** is defined as follows

$$S=\begin{bmatrix} EA & 0 & 0 \\ 0 & GA & 0 \\ 0 & 0 & EI \end{bmatrix} \tag{A4}$$

$\mathbf{B}_m$ matrix is as follows

$$\mathbf{B}_m=\mathbf{B}\Big|_{\xi=0}=\frac{1}{L_0}\begin{bmatrix} -c_m & -s_m & -\frac{1}{2}L_0\gamma_m & c_m & s_m & -\frac{1}{2}L_0\gamma_m \\ s_m & -c_m & \frac{1}{2}L_0(1+e_m) & s_m & -c_m & \frac{1}{2}L_0(1+e_m) \\ 0 & 0 & -1 & 0 & 0 & 1 \end{bmatrix} \tag{A5}$$

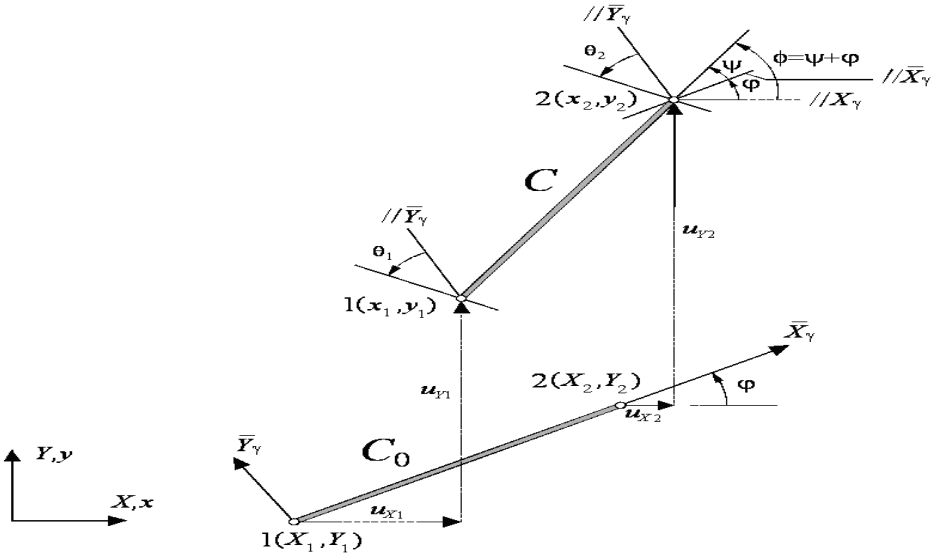

Fig. A1 Plane beam element with arbitrarily oriented reference configuration (Felippa 2014) The geometric stiffness matrix K_G is given as follows

$$K_G = \frac{N_m}{2}\begin{bmatrix} 0 & 0 & s_m & 0 & 0 & s_m \\ 0 & 0 & -c_m & 0 & 0 & -c_m \\ s_m & -c_m & -\frac{1}{2}L_0(1+e_m) & -s_m & c_m & -\frac{1}{2}L_0(1+e_m) \\ 0 & 0 & -s_m & 0 & 0 & -s_m \\ 0 & 0 & s_m & 0 & 0 & c_m \\ s_m & -c_m & -\frac{1}{2}L_0(1+e_m) & -s_m & c_m & -\frac{1}{2}L_0(1+e_m) \end{bmatrix}$$

$$+\frac{V_m}{2}\begin{bmatrix} 0 & 0 & c_m & 0 & 0 & c_m \\ 0 & 0 & s_m & 0 & 0 & s_m \\ c_m & s_m & -\frac{1}{2}L_0\gamma_m & -c_m & -s_m & -\frac{1}{2}L_0\gamma_m \\ 0 & 0 & -c_m & 0 & 0 & -c_m \\ 0 & 0 & -s_m & 0 & 0 & -s_m \\ c_m & s_m & -\frac{1}{2}L_0\gamma_m & -c_m & -s_m & -\frac{1}{2}L_0\gamma_m \end{bmatrix} \tag{A6}$$

in which N_m and V_m are the axial and shear forces which are evaluated at the midpoint. The internal nodal force vector is as follows Felippa (2014)

$$\mathbf{p} = L_0 \mathbf{B}_m^T \mathbf{z} = \begin{bmatrix} -c_m & -s_m & \frac{1}{2}L_0\gamma_m & c_m & s_m & \frac{1}{2}L_0\gamma_m \\ s_m & c_m & -\frac{1}{2}L_0(1+e_m) & s_m & -c_m & -\frac{1}{2}L_0(1+e_m) \\ 0 & 0 & -1 & 0 & 0 & 1 \end{bmatrix}^T \begin{bmatrix} N \\ V \\ M \end{bmatrix} \tag{A7}$$

where $\mathbf{z}^T=[N\ V\ M]$. The external nodal force vector can be expressed as follows

$$f = b\int_h \int_{L_0} \begin{bmatrix} 1-\xi_1 & 0 & 0 \\ 0 & 1-\xi_1 & 0 \\ 0 & 0 & 1-\xi_1 \\ 1-\xi_2 & 0 & 0 \\ 0 & 1-\xi_2 & 0 \\ 0 & 0 & 1-\xi_2 \end{bmatrix} \begin{bmatrix} f_X \\ f_Y \\ 0 \end{bmatrix} dXdY + b\int_{L_0} \begin{bmatrix} 1-\xi_1 & 0 & 0 \\ 0 & 1-\xi_1 & 0 \\ 0 & 0 & 1-\xi_1 \\ 1-\xi_2 & 0 & 0 \\ 0 & 1-\xi_2 & 0 \\ 0 & 0 & 1-\xi_2 \end{bmatrix} \begin{bmatrix} t_X \\ t_Y \\ t_Z \end{bmatrix} dX \tag{A8}$$

where f_X, f_Y are the body forces, t_X, t_Y, m_Z are the surface loads in the X, Y directions and about the Z axis.